European Journal of Radiology 79 (2011) e24–e27

Contents lists available at ScienceDirect

European Journal of Radiology

journal homepage: www.elsevier.com/locate/ejrad

Detection accuracy of *in vitro* approximal caries by cone beam computed tomography images

Xingmin Qu, Gang Li*, Zuyan Zhang, Xuchen Ma

Department of Oral and Maxillofacial Radiology, Peking University School and Hospital of Stomatology, #22 Zhongguancun Nandajie, Hai Dian District, Beijing 100081, China

ARTICLE INFO

Article history:
Received 5 May 2009
Accepted 6 May 2009

Keywords:
Approximal caries
Diagnostic accuracy
CBCT
Detector type
FOV
ROC analysis

ABSTRACT

Aims: To evaluate the diagnostic accuracy of approximal carious lesions among five CBCT systems and to assess the effect of detector types employed by different CBCT systems on the accuracy of approximal caries diagnosis.
Materials and methods: Thirty-nine extracted non-cavitated human permanent teeth were employed in the study. Seven observers evaluated 78 approximal surfaces of the teeth with respect to caries by the images from the following five CBCT systems: (1) NewTom 9000; (2) Accuitomo 3DX; (3) Kodak 9000 3D; (4) ProMax 3D; and (5) DCT PRO, respectively. The lesions were validated by histological examination. The area under receiver operating characteristic (ROC) curve (A_z) was used to evaluate the diagnostic accuracy.
Results: Microscopy of approximal surfaces found 47.4% sound, 39.8% enamel and 12.8% dentin lesions. The differences of A_z values among the five CBCT systems were not statistically significant ($p = 0.348$). No significant difference was found between the two detector types of CBCT systems ($p = 0.47$).
Conclusions: The five CBCT systems employed in the study showed no significant difference in the *in vitro* approximal caries detection. Neither the detector nor the FOV employed by the CBCT systems has an impact on the detection accuracy of approximal caries.

1. Introduction

Approximal tooth surfaces can hardly be approached or visualized directly and therefore approximal caries are often diagnosed with the aid of radiographs. The most widely used clinical technique for the diagnosis of approximal carious lesions is bitewing radiography. However, the reported sensitivity and specificity of this method were rather low in some studies [1–3]. Thus, alternative technologies for detecting approximal caries, such as digital radiography [4] and ultrasonic caries detector [5], were introduced. However, the results were not satisfying.

Cone beam computed tomography (CBCT) is a new technology that can provide sagittal, coronal and axial images with sub-millimeter resolutions. The radiation dose is lower than conventional CT [6]. CBCT has been used in several dental diagnostic areas including implant placement [7], temporomandibular joint examination [8], endodontic treatment [9], orthodontics [10] and periodontology [11]. Moreover, CBCT appears to be a promising tool for assessing already-observed small carious lesions [12] and the hidden caries beneath a sound surface [13]. However, the diagnostic accuracy of CBCT for approximal caries is controversial [14–16].

Currently, there are two types of image detectors employed by CBCTs. One is the Image Intensifier + Charge Coupled-Device (II + CCD) and the other is the flat panel detector including Amorphous silicon Flat Panel (AFP) and Complementary Metal Oxide Semiconductor Flat Panel (CMOS FP). Although many studies have been performed to validate the diagnostic efficacy and efficiency for caries detection [10–14], the differences on diagnostic accuracy of the CBCT systems with these two types of detector have not been so far evaluated.

Thus, the aims of the present study were: (1) to evaluate the diagnostic accuracy of approximal carious lesions among five CBCT systems; (2) to assess the effect of detector types employed by different CBCT systems on the accuracy of approximal caries diagnosis.

2. Materials and methods

2.1. Teeth

A total of 39 non-cavitated human permanent teeth extracted from 11 excised jaws were employed in the present study. The clinical appearance of the tooth surface after cleaning ranged from sound to discolored, with white/brown discolorations. The teeth

* Corresponding author. Tel.: +86 10 62179977x2328; fax: +86 10 62179977x2328.
E-mail addresses: quxingmin@bjmu.edu.cn (X. Qu), kqgang@bjmu.edu.cn (G. Li), zhangzy-bj@vip.sina.com (Z. Zhang), kqxcma@bjmu.edu.cn (X. Ma).

0720-048X/$ – see front matter © 2010 Elsevier Ireland Ltd. All rights reserved.
doi:10.1016/j.ejrad.2009.05.063

Table 1
Overview of the CBCT devices and the selected scan protocols.

CBCT device	kV	mA	Scanning time (s)	Detector	FOV (cm)	Voxel size (mm)	Slice thickness (mm)
NewTom 9000	110	2.1	36	II + CCD	15 × 15	0.3	0.4
Accuitomo 3DX	80	5	17.5	II + CCD	3 × 4	0.125	1
Kodak 9000 3D	70	10	24	AFP	5 × 3.7	0.076	0.076
ProMax 3D	76	6	18	CMOS FP	8 × 8	0.32	0.32
DCT PRO	90	3.5	24	CMOS FP	20 × 19	0.322	1

were mounted in 11 plaster blocks, with the prominent part of the approximal surfaces in contact and at the same vertical level, simulating the normal anatomical position. The 11 tooth blocks were numbered and stored separately in 10% neutral buffered formalin solution.

2.2. CBCT scanning

CBCT data of the 11-block samples were acquired with five CBCT scanners: NewTom 9000® (Quantitative Radiology, Verona, Italy), Accuitomo 3DX® (J.MORITA, Mfg, Corp., Kyoto, Japan), Kodak 9000 3D® (Carestream Health, Inc., New York, USA), ProMax 3D® (Planmeca Oy, Helsinki, Finland), DCT PRO® (VATECH, Co., Ltd., Yongin-Si, S. Korea). The CBCT specifications and scanning protocols for each scanner are shown in Table 1. During the CBCT exposures, a 20-mm thick water phantom was placed around the blocks to simulate soft tissues.

2.3. CBCT images

The CBCT images were subsequently reconstructed by the proprietary software of each system except for the NewTom 9000. For the NewTom 9000, the raw data from each tooth block were exported by the proprietary software NewTom 3.10. The primary and secondary reconstructions were then performed by the NewTom 3G software package NNT2.17 (Quantitative Radiology, Verona, Italy). Each tooth was sectioned in the mesiodistal direction with the minimal slice thickness of each system (Table 1). The mesiodistal images of all teeth were exported from the systems and saved as bitmap (BMP) format. Example image is shown in Fig. 1.

2.4. Viewing

With respect to the approximal carious lesions, seven observers who had experience of caries diagnosis evaluated all the test images twice. There was at least 1 week separation between the first and second evaluations. The images were displayed in a random order for each observer. The monitor employed was a 22-inch Dell™ E228WFP flat panel monitor with a resolution of 1680 × 1050 pixels. To display the images in a series order, the software package ACDsee v10.0 (ACD Systems International Inc., British Columbia, Canada) was employed. Viewing took place in a room with dimmed light. Prior to observation, one of the investigators calibrated the monitor with the SMPTE pattern included in the software DentalEye 3.0 (DentalEye AB, Sundbyberg, Sweden). No extra adjustment of brightness and contrast was allowed. The display ratio of the images was 1:1. The following 5-point rank scale was employed for the observers to record their level of confidence on approximal carious lesions: 1 = definitely no caries; 2 = probably no caries; 3 = questionable; 4 = probably caries; 5 = definitely caries.

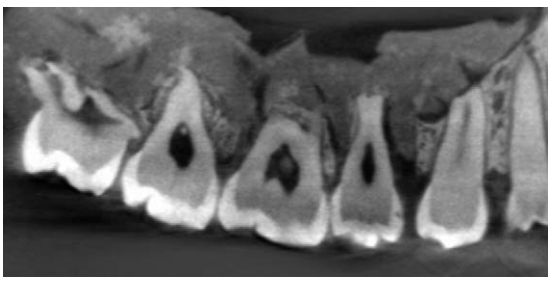

Fig. 1. Example image obtained from one of studied CBCT imaging systems.

2.5. Histological validation

For the validation of the true presence of caries, the teeth were individually embedded in polyacrylic resin and serially sectioned (700-μm-thick sections) in the mesiodistal direction using an Isomet® Low Speed Saw (Buehler Ltd., IL, USA) with a 200-μm diamond saw blade. The tooth sections were validated with a 16× magnifying stereomicroscope ZOOM-630E (Changfang Optical Instrument Ltd., Shanghai, China) by two investigators. Approximal carious lesion, defined as an opaque-white demineralization or brownish discoloration observed in the approximal surface was scored on the following scale: 0 = sound, 1 = caries in enamel, 2 = caries reaching but not crossing the enamel dentine junction (EDJ) and 3 = caries into dentine. The highest score from the various sections of an approximal surface was defined as the true status for the assessed surface. In case the observers' ratings varied, they performed a joint assessment to establish agreement.

2.6. ROC analysis

With the histological examination as gold standard, each observer's performance was subsequently converted into a receiver operating characteristic (ROC) curve with the program SPSS-version 11.0 for Windows (SPSS Inc., Chicago, IL, USA). The maximum likelihood parameters were determined and the area under the ROC curve (A_z) was calculated.

2.7. Statistical analysis

Repeated-measure ANOVA was employed to analyze the A_z values from each observer and inter-observer variances. Intra-observer variance was analyzed by Student's *t*-test. A significant difference was considered when $p < 0.05$.

3. Results

Histological examination revealed that of the 78 approximal surfaces, 37 were sound, 24 showed enamel caries, 7 had caries reaching the EDJ and 10 had dentin caries (Table 2).

Table 2
True status of the tooth surfaces according to histological examination.

	No. of tooth surfaces	%
Sound surfaces	37	47.4
Enamel carious surfaces	24	30.8
Caries reaching EDJ	7	9.0
Dentin caries	10	12.8
Total	78	100

Table 3
Areas under receiver operating characteristic curves (A_z) from each observer.

Observer	NewTom 9000	Accuitomo 3DX	Kodak 9000 3D	ProMax 3D	DCT PRO
1	0.559	0.473	0.545	0.580	0.532
2	0.590	0.530	0.640	0.550	0.530
3	0.563	0.590	0.539	0.560	0.557
4	0.502	0.592	0.614	0.529	0.564
5	0.550	0.561	0.571	0.516	0.554
6	0.506	0.592	0.576	0.520	0.598
7	0.519	0.544	0.552	0.557	0.512
Mean	0.541	0.555	0.577	0.545	0.549
SD	0.033	0.044	0.038	0.024	0.028

SD, standard deviation.

Table 4
p-Values for observer performance from each CBCT system.

	Accuitomo 3DX	Kodak 9000 3D	ProMax 3D	DCT PRO
NewTom 9000	0.666	0.083	0.718	0.726
Accuitomo 3DX		0.280	0.773	0.740
Kodak 9000 3D			0.148	0.143
ProMax 3D				0.790

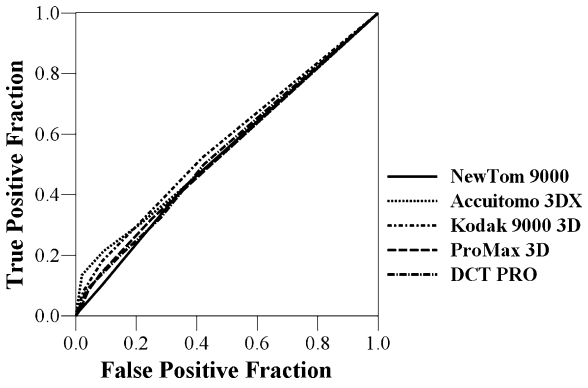

Fig. 2. ROC curve from combined observer performance.

Table 3 shows the area under ROC curve from each observer. The mean A_z value for Kodak 9000 3D was a little bit larger than those for other systems. Significant differences were not found among the five CBCT systems ($p = 0.348$). Pair wise comparison of the observer performance from each CBCT system is shown in Table 4.

The mean A_z value for Kodak 9000 3D, ProMax 3D and DCT PRO was 0.557 while the mean for NewTom 9000 and Accuitomo 3DX was 0.548. No significant difference was found between the two types of CBCT detectors ($p = 0.47$).

There is no significant difference on inter- and intra-observer variances for detecting approximal caries ($p = 0.744$ and 0.219, respectively).

Fig. 2 demonstrates the ROC curves obtained from combined observer performance.

4. Discussion

Due to the nature of CBCT images, CBCT appears to be a promising tool for caries diagnosis. However, the diagnostic accuracy of CBCT for approximal carious lesion was controversial. The work performed by van Daatselaar and coworkers demonstrated the superiority of CBCT images over conventional 2D radiographs for approximal caries detection [14,15] while other researchers found no differences or lower diagnostic accuracy [16]. This may relate to the fact that the evaluating algorithms employed in the studies were different.

An objective comparison of diagnostic accuracy of imaging systems requires a simultaneous evaluation of sensitivity and specificity [17]. ROC analysis, developed to evaluate the quality of signal detection by observers responding to stimuli in an environment of varying levels of noise, is a method that evaluates sensitivity and specificity simultaneously [18]. This method is a least biased measure of diagnostic performance. ROC curve graphically presents the ratio of the sensitivity and false sensitivity responses as a decision criterion is varied. The most common index to characterize an ROC curve is the A_z value, i.e. the area under the ROC curve. This value may vary from 0.5 to 1.0, in which 0.5 represents a random decision and 1.0 a perfect diagnostic justification [19]. ROC analysis yields valid measurements of observer performance in diagnostic tasks pertaining to the detection of carious lesions by radiography [20].

The present study revealed that the diagnostic accuracy defined by A_z values of the five CBCT systems were very similar, 0.541 for the NewTom 9000, 0.555 for the Accuitomo 3DX, 0.577 for the Kodak 9000 3D, 0.545 for the ProMax 3D and 0.549 for the DCT PRO. These values were low and did not indicate a good diagnostic accuracy. The explanation for the low values is that only non-cavitated teeth were employed in the present study. In fact, these values were very typical for enamel caries observed in film and digital radiographs [21]. This may indicate that with regard to non-cavitated approximal caries, the diagnostic accuracy may not be improved by the CBCT imaging modality. This was supported by the studies of Tsuchida [22] and Akdeniz [12].

The detectors employed by the studied CBCT systems were not the same. The NewTom 9000 and the Accuitomo 3DX employed a detector of II and CCD type while the other three systems employed a type of flat panel detector composed of Amophors Silicon or CMOS. However, the diagnostic accuracy as defined by the A_z values demonstrated no significant differences among the five CBCT systems. When the observer performance was analyzed according to detector types employed by the CBCT systems, the difference between the two types of CBCT detectors was not significant ($p = 0.47$), neither, despite of the mean A_z value (0.557) for the flat panel systems was little bit larger than that (0.548) for the II + CCD type systems. This may reveal that with regard to the approximal caries detection, the detector types employed by the CBCT systems have no effect on the accuracy of approximal caries diagnosis.

In the present study, the fields of view (FOVs) of the employed CBCT systems were different. The CBCT system DCT PRO has a large FOV that is up to 20 cm × 19 cm while the Accuitomo 3DX and the Kodak 9000 3D have a relative small FOV of around 3 cm × 4 cm. In principle, the CBCT system creates a smaller image of the same region of interest with a large FOV than with a small FOV. Thus, when the images are displayed in 1:1 ratio, the images of teeth obtained from the Accuitomo 3DX and the Kodak 9000 3D are larger than those obtained from the other three systems. However, the present study did not show any difference among the systems with respect to the approximal caries detection.

The slice thickness of one reconstructed image may have an influence on the diagnostic accuracy. This may be true for a conventional CT image that is obtained from a fan beam projection. For a cone beam CT, the geometry is volumetric and thus the reconstructed images display the studied entity in a continuous way and without any possibility of omitting small disease between two image layers. To reveal the maximum capability of one CBCT system for approximal caries detection, the images in the present study were reconstructed to the smallest thickness that one system can generate.

5. Conclusions

The CBCT systems employed in the present study demonstrated no significant difference on the detection of *in vitro* approximal caries. Neither the detector nor the FOV employed by the CBCT systems has an impact on the detection of approximal caries.

Acknowledgements

We wish to express our sincere appreciations to Dr. Ling Xiao and Prof. Yucheng Su for allowing us to use their CBCT units and to all the observers who have assessed the CBCT images.

References

[1] Wenzel A. Bitewing and digital bitewing radiography for detection of caries lesions. J Dent Res 2004;83:C72–5. Spec No. C.
[2] White SC, Yoon DC. Comparative performance of digital and conventional images for detecting proximal surface caries. Dentomaxillafac Radiol 1997;26:32–8.
[3] Ludlow JB, Platin E, Delano EO, Clifton L. The efficacy of caries detection using three intraoral films under different processing conditions. J Am Dent Assoc 1997;128:1401–8.
[4] Shi XQ, Li G. Detection accuracy of approximal caries by black-and-white and color-coded digital radiographs. Oral Surg Oral Med Oral Pathol Oral Radiol Endod 2009;107:433–6.
[5] Matalon S, Feuerstein O, Calderon S, Mittleman A, Kaffe I. Detection of cavitated carious lesions in approximal tooth surfaces by ultrasonic caries detector. Oral Surg Oral Med Oral Pathol Oral Radiol Endod 2007;103:109–13.
[6] Tsiklakis K, Donta C, Gavala S, et al. Dose reduction in maxillofacial imaging using low dose Cone Beam CT. Eur J Radiol 2005;56:413–7.
[7] Madrigal C, Ortega R, Meniz C, López-Quiles J. Study of available bone for interforaminal implant treatment using cone-beam computed tomography. Med Oral Pathol Oral Cir Bucal 2008;13:E307–12.
[8] Tsiklakis K, Syriopoulos K, Stamatakis HC. Radiographic examination of the temporomandibular joint using cone beam computed tomography. Dentomaxillofac Radiol 2004;33:196–201.
[9] Matherne RP, Angelopoulos C, Kulild JC, Tira D. Use of cone-beam computed tomography to identify root canal systems in vitro. J Endod 2008;34:87–9.
[10] Korbmacher H, Kahl-Nieke B, Schöllchen M, Heiland M. Value of two cone-beam computed tomography systems from an orthodontic point of view. J Orofac Orthop 2007;68:278–89.
[11] Noujeim M, Prihoda T, Langlais R, Nummikoski P. Evaluation of high-resolution cone beam computed tomography in the detection of simulated interradicular bone lesions. Dentomaxillofac Radiol 2009;38:156–62.
[12] Akdeniz BG, Gröndahl HG, Magnusson B. Accuracy of proximal caries depth measurements: comparison between limited cone beam computed tomography, storage phosphor and film radiography. Caries Res 2006;40:202–7.
[13] Haiter-Neto F, Wenzel A, Gotfredsen E. Diagnostic accuracy of cone beam computed tomography scans compared with intraoral image modalities for detection of caries lesions. Dentomaxillofac Radiol 2008;37:18–22.
[14] van Daatselaar AN, Dunn SM, Spoelder HJ, et al. Feasibility of local CT of dental tissues. Dentomaxillofac Radiol 2003;32:173–80.
[15] van Daatselaar AN, Tyndall DA, van der Stelt PF. Detection of caries with local CT. Dentomaxillofac Radiol 2003;32:235–41.
[16] Kalathingal SM, Mol A, Tyndall DA, Caplan DJ. In vitro assessment of cone beam local computed tomography for proximal caries detection. Oral Surg Oral Med Oral Pathol Oral Radiol Endod 2007;104:699–704.
[17] Berkey CS, Douglass CW, Valachovic RW, Chauncey HH, McNeil BJ. Statistical methods for comparing dental diagnostic procedures. Community Dent Oral Epidemiol 1990;18:169–76.
[18] Obuchowski NA. Receiver operating characteristic curves and their use in radiology. Radiology 2003;229:3–8.
[19] Sanderink GC, Huiskens R, van der Stelt PF, Welander US, Stheeman SE. Image quality of direct digital intraoral X-ray sensors in assessing root canal length. The RadioVisioGraphy, Visualix/VIXA, Sens-A-Ray, and Flash Dent systems compared with Ektaspeed films. Oral Surg Oral Med Oral Pathol 1994;78:125–32.
[20] Verdonschot EH, Wenzel A, Bronkhorst EM. Applicability of Receiver Operating Characteristic (ROC) analysis on discrete caries depth ratings. Community Dent Oral Epidemiol 1993;21:269–72.
[21] Castro VM, Katz JO, Hardman PK, Glaros AG, Spencer P. In vitro comparison of conventional film and direct digital imaging in the detection of approximal caries. Dentomaxillofac Radiol 2007;36:138–42.
[22] Tsuchida R, Araki K, Okano T. Evaluation of a limited cone-beam volumetric imaging system: comparison with film radiography in detecting incipient proximal caries. Oral Surg Oral Med Oral Pathol Oral Radiol Endod 2007;104:412–6.